Pickering particle and emulsifier co-stabilised emulsions produced via rotating membrane emulsification

Arkoumanis, Panagiotis G.; Norton, Ian T.; Spyropoulos, Fotis

DOI:
10.1016/j.colsurfa.2019.02.036

Document Version
Peer reviewed version

Citation for published version (Harvard):
Arkoumanis, PG, Norton, IT & Spyropoulos, F 2019, 'Pickering particle and emulsifier co-stabilised emulsions produced via rotating membrane emulsification', *Colloids and Surfaces A: Physicochemical and Engineering Aspects*, vol. 568, pp. 481-492. https://doi.org/10.1016/j.colsurfa.2019.02.036

Pickering particle and emulsifier co-stabilised emulsions produced via rotating membrane emulsification

Panagiotis G. Arkoumanis*, Ian T. Norton, Fotis Spyropoulos

School of Chemical Engineering, University of Birmingham, Edgbaston B15 2TT, UK

Keywords: Pickering emulsion; edible particle; protein; surfactant; co-stabilisation; rotating membrane

* Corresponding author: *Email address*: pga441@bham.ac.uk

Abstract:

Producing stable particle-stabilised emulsions of small droplet sizes and high monodispersity via membrane emulsification approaches is hindered by the poor mixing environment during processing and the low diffusivity and minimal interfacial tension lowering capacity of colloidal particles. The present study investigates the co-stabilisation (particles and emulsifiers) of O/W emulsions formed by rotating membrane emulsification. Formulation aspects of the employed co-stabilisation strategy (type/concentration of emulsifiers and type/size of particles) were assessed at a fixed trans-membrane pressure (10 kPa) and rotational velocity (2000 rpm). Emulsion microstructure was shown to be affected by the occurrence of emulsifier/particle interactions. In formulations where these interactions are synergistic and emulsifier content is low, interfacial stabilisation is carried out by both species and resulting emulsions possess smaller droplet sizes, higher monodispersity indices and enhanced stability against coalescence, compared to systems stabilised by either of the two components alone. This work concludes that a carefully controlled co-stabilisation strategy can overcome the current challenges associated with the production of particle-stabilised emulsions via membrane emulsification methods.

1. Introduction

The incorporation of one phase into another immiscible phase is the basis of the microstructure of many emulsion-based products. A variety of emulsification processes have been developed to deliver this microstructure which usually requires high energy dissipation to effectively breakup droplets to a finite size thereby improving stability and overall quality of the finished product [1]. However, the high mechanical stresses generated by these processes may be unfavourable in the case of sensitive ingredients (e.g. bioactives) incorporated in the system thus making them less functional. Additionally, the repeated random breakup of droplets can increase re-coalescence rates and hence emulsion polydispersity [2]. What is more, emulsification techniques based on comminution are typically associated with high energy inputs and significantly low energy efficiencies [3].

Membrane emulsification (ME) is a promising technique that requires a much lower energy input compared to traditional emulsification methods, whilst at the same time produces emulsions with low polydispersity [4, 5]. Droplets are formed one-at-the-time by introducing the to-be-dispersed phase through a porous membrane into the external continuous and in response to a number of forces acting on the developing droplet [5]. Droplet size can be tuned depending on process conditions (e.g. transmembrane pressure, rotational velocity), formulation characteristics (surfactant/stabiliser type and concentration, dispersed phase fraction) and membrane properties (pore size, porosity, hydrophilicity/hydrophobicity) [6]. Several configurations of membrane emulsification have been identified including cross-flow, stirred vessel, vibrating and pulsed membrane set-ups [7]. The advantage of rotating membrane emulsification (RME) against other process configurations primarily stems from the additional centrifugal force exerted on the emerging phase, which not only promotes earlier detachment but also assists in moving formed droplets away from the membrane surface [8].

Because of the crucial role of emulsifiers in aiding droplet detachment, current membrane emulsification literature is primarily focused on emulsions produced in the presence of such surface active species and studies investigating alternative emulsion stabilisation approaches, such as Pickering stabilisation, are limited. Pickering emulsions have received great attention in literature predominantly due to their superior stability and the Pickering functionality of a range of colloidal particles (including species formed from edible sources) has been extensively studied [9-12]. However, the vast majority of Pickering emulsion literature focuses on the utilisation of conventional high energy input emulsification methods. The reason for this is that ME operation is not well placed to facilitate particle adsorption at the oil/water interface and

thus emulsion stability is either compromised or is achieved at the expense of large emulsion droplet sizes.

Conversely to classic emulsifiers that spontaneously adsorb at an interface through diffusion, colloidal particles need to possess adequate kinetic energy to initially be transferred via convection to the droplet subsurface and from there to finally overcome the energy barrier associated with their adsorption at the oil/water surface [13, 14]. Particle wettability (contact angle) and size will then determine whether adsorption will be irreversible [15]. Due to its low-energy input and poor mixing environment, the RME (and ME in general) operation does not encourage particle transfer towards the droplet subsurface and thus Pickering stabilisation is significantly delayed and often ineffective. In recent studies, the stability and droplet size of emulsions prepared with silica and latex nanoparticles and processed with a rotating membrane device was investigated [16, 17]. The authors reported large droplet sizes and enhanced coalescence phenomena, which were attributed to the fact that the critical time for adsorption of particles at the interface was higher than the droplet formation time.

A feasible strategy to enhance the Pickering stabilisation of emulsions produced by high shear methods has been to combine colloidal particles with emulsifiers [18, 19]. For example, in both silica particles/Tween 20 [20] and hydroxypropyl methyl cellulose particles/Tween 60 [21] co-stabilisation approaches, advances in Pickering stabilisation under high shear mixing were indeed reported but only at a low emulsifier content. Despite its relative prevalence in emulsions formed by high shear techniques, the utilisation of a co-stabilisation strategy in ME has only been reported once. Co-stabilised O/W Pickering emulsions were produced by RME using a laser-drilled stainless membrane and silica and latex particles in combination with a variety of low molecular weight (LMW) emulsifiers [22]. The authors reported co-stabilisation by either competitive (no interaction between the two species) or synergistic adsorption (electrostatic and/or hydrophobic attraction between species) onto oil droplets.

The present study aims to extend the currently limited scientific understanding on the effectiveness of co-stabilisation approaches in O/W emulsions produced by RME. The strategy employed here is devised to assess for the first time the effectiveness of a protein (whey protein isolate) as the emulsifier species within the co-stabilisation formulation and compare it to the behaviour of a small molecular weight emulsifier (Tween 20). Emulsions are formed using a RME device in the presence of either emulsifier (Tween 20 or WPI) together with two types of colloidal particles (silica or hydroxypropyl methyl cellulose particles) of demonstrated Pickering functionality [20, 21, 23]. The effectiveness of the co-stabilisation approach was

assessed at a fixed trans-membrane pressure of 10 kPa and a constant rotational velocity of 2000 rpm. Formulation aspects of the co-stabilisation strategy were related to the droplet size, droplet size distribution and coalescence stability over time (up to three weeks) of the produced emulsions. Only considering Pickering emulsions produced under the same RME processing conditions, co-stabilised systems with only a 0.05 wt.% emulsifier content are shown to produce emulsions of much lower droplet sizes (20 μm rather than 40 μm), higher monodispersity (span value of 0.7 as oppose to 2) and enhanced long term stability.

Materials and methods

2.1. Materials

Emulsions were made from distilled water (de-ionised and filtrated in a reverse osmosis unit) and commercial sunflower oil with a viscosity of 0.066 Pa s and density 915 kg m^{-3} (purchased from the local store). Particles used as Pickering stabilisers were Ludox SM colloidal silica provided in aqueous suspension 30 wt.%, and hydroxypropyl methyl cellulose powder (HPMC, $M_n \approx 10000$) purchased from Sigma-Aldrich, UK [24]. Polysorbate 20 (Tween 20) was used as LMW emulsifier and was purchased from Sigma- Aldrich, UK as a yellow viscous liquid. Whey protein isolate (WPI) was used as high molecular weight (HMW) emulsifier and was purchased in white powder form from Volac UK with a bulk density of 0.43 g/ml and 5.5% moisture. Sodium azide was purchased from Sigma-Aldrich UK. Hydrochloric acid (HCl 30 wt.% solution) and sodium hydroxide (NaOH pellets) were also purchased from Sigma - Aldrich UK.

2.2. Methods

2.2.1. Preparation of aqueous phase

Solutions of emulsifiers were made by dissolving the required amount of Tween 20 or WPI in distilled water whilst agitating gently with a magnetic stirrer overnight. Suspensions of silica particles were prepared by diluting the original suspension with distilled water to the desired concentration and the pH was adjusted to 2 to decrease the surface charge of particles and enable them to pack closely once they adsorb to oil droplet surface in order to prevent destabilisation. Suspensions of HPMC were made by dissolving the powder in distilled water. HPMC is a non-ionic polysaccharide and its charge is not expected to be affected substantially by the pH, thus the native pH (~ 6.5) was used. HPMC suspensions were heated at 45°C for 45-50 minutes whilst agitating with a magnetic stirrer. This process would allow

for dispersion of the powder avoiding aggregation/ gelation (T_{gel}= 58 - 64°C according to manufacturer's data). Following this, they were processed in batches of 80 g with an ultrasonic probe (VC750 Ultrasonic Vibra-Cell processor, Sonics & Materials Inc, USA) at 20 kHz for 2 minutes and they were left stirring until cooled down to ambient temperature. The aqueous mixtures of particles and Tween 20 were prepared by adding the appropriate amount of Tween 20 in the particle suspension followed by ultrasound treatment as described previously. For the preparation of the mixtures of particles and WPI, the particles were added in the WPI solution, followed by ultrasound. Prior to ultrasound, the pH of the mixtures containing silica particles and HPMC particles was adjusted to 2 and 6.5 respectively. Stock solutions of HCl and NaOH 0.5M and 1M were prepared and where necessary, the pH of the aqueous phase was adjusted. For all aqueous phases containing WPI, sodium azide was used at a concentration of 0.01 wt.% to prevent bacterial growth. A summary of species used in mixtures with water are given in Table1.

Table 1: Composition of aqueous phase. Concentration of all particles was 3 wt.% in all cases. Concentrations are in wt.%: weight of individual species over the weight of the final emulsion.

Aqueous phase	Abbreviation
3% Silica	S
3% HPMC	H
0.05% Tween 20	0.05T
3% Tween 20	3T
0.05% WPI	0.05W
3% WPI	3W
3% Silica / 0.05% Tween 20	S / 0.05T
3% Silica / 3% Tween 20	S / 3T
3% Silica / 0.05% WPI	S / 0.05W
3% Silica / 3% WPI	S / 3W
3% HPMC / 0.05% Tween 20	H / 0.05T
3% HPMC / 3% Tween 20	H / 3T
3% HPMC / 0.05% WPI	H / 0.05W
3% HPMC / 3% WPI	H / 3W

2.2.2. Rotating Membrane Emulsification (RME)

The operation and the configuration of RME have been extensively described previously [25]. Oil-in-water emulsion batches of 110 g containing 10 wt.% oil were produced in all cases in a 150 ml beaker. A hydrophilic tubular Shirasu porous glass membrane (SPG Technology Co. Ltd, Japan) was used with average pore diameter 6.1 μm, average porosity 0.56 - 0.58 [26], wall thickness of 1mm, length 45 mm and outer diameter 10 mm, according to manufacturer's

data. The sunflower oil was pushed through the membrane in the aqueous phase at a constant trans-membrane pressure 10 kPa whilst maintaining constant rotational velocity at 2000 rpm corresponding to a shear rate of 14 s^{-1}.

2.2.3. Analytical techniques

2.2.3.1. Particle and emulsion droplet size measurements

The particle size of aqueous suspensions and emulsion droplet size were determined by static multi-angle light scattering (SMLS) using a Mastersizer (Malvern Instruments, UK) with a Hydro 2000 SA suspension cell unit. For aqueous suspensions containing species < 1 μm a Zetasizer Nano ZS (Malvern Instruments. UK) was used deploying dynamic light scattering (DLS). The refractive index (RI) used for the mixed particle-emulsifier suspensions was the RI of the particles. Particle size measured with Zetasizer was expressed as the Z-average or cumulants mean while the polydispersity index (PDI) was used to describe the width distribution. All emulsions produced via RME presented monomodal distribution, therefore emulsion droplet size was expressed as D_{43} (volume weighted mean) and the value of span represented the width of the distribution.

$$Span = \frac{D_{90} - D_{10}}{D_{50}} \quad (1)$$

where D_n (n= 1-100) indicates the volume diameter of which n% of the volume distribution is below this value. Stability of the emulsions was evaluated by measuring emulsion droplet size and span for 21 days.

2.2.3.2. Zeta potential measurements

Zeta-potential and Z-average size of all particle suspensions were simultaneously recorded using an MPT-2 Titrator attached to the Zetasizer main unit. Prior to the titration, the samples were prepared at native pH and the pH was adjusted with 0.1M HCl and NaOH solutions as titrants.

2.2.3.3. Microstructure visualisation

Images of oil droplets and the membrane surface were captured by a light microscope (Leica DM 2500 LED). A drop of each emulsion sample was placed on a thin glass slide under the microscope and analysed in different magnifications. Membranes were placed directly under the microscope and light was illuminated properly towards the surface to obtain a clear view

of the pores. Cryogenic scanning electron microscopy (Cryo-SEM; Philips XL30 FEG ESSEM) was also used to visualise oil droplet surface. One drop of the emulsion was placed on a sample holder and was frozen to -173 °C with liquid nitrogen. Then the sample was transferred to a preparation chamber; the heating was turned on to reach a temperature of -90 °C and the samples were fractured under vacuum in order to remove water components. The heating was turned off, and the samples were dusted with gold particles and scanned whilst maintaining the temperature at -140°C with the addition of liquid nitrogen.

2.2.3.4. Viscosity measurements

The apparent viscosity of the aqueous suspensions was measured as function of shear rate with a Kinexus Pro rotational rheometer (Malvern Instruments, UK). A cup and bob geometry was used at 20°C for a range of shear rates between 0.1 and 100 s^{-1}.

2.2.3.5. Statistical analysis

Analysis of variance (one-way Anova) was performed to evaluate significant differences between the measurements with regards to zeta potential and particle size (obtained from DLS). Data were checked for normal distribution and equality of variance before analysis of variance whilst Tukey's HSD test was deployed for multiple comparisons of means. Significance was chosen as $p < 0.05$. The statistical analysis was performed using SPSS software package (IBM SPSS Statistics, US). All emulsion data plotted in the present work are averaged values of a triplicate of measurements provided as: $\mu \pm 2$ s (μ: average value, and s: standard deviation). The same approach was taken for the calculation of the error bars shown in all figures. Data is expected to be within this range ($\mu \pm 2$ s) with a confidence of more than 95%.

3. Results and discussion

3.1. Particle and mixed particle-emulsifier aqueous suspensions

The coexistence of particles and classic emulsifiers in the aqueous phase could trigger electrostatic and/or hydrophobic interactions between the species owing to the surface chemistry of each entity and this could affect emulsification and emulsion stability [9, 27]. An increase of the particle size and/ or the increase of the zeta potential of particles towards a net value upon addition of emulsifiers could be a valid indication that interactions occur between the species. For example in the work of Binks et al. the adsorption of a cationic surfactant

(CTAB) to silica nanoparticles was accompanied by an increase in the magnitude of the zeta potential from negative to positive value [23]. However, it is rather difficult to identify precisely the type and strength of underlying interactions in such systems; therefore, a combined approach was used to describe the events based on the available characterisation data. The particle size and the zeta potential of species alone and mixed in water was measured (Table 2). In general, it can be seen that for aqueous suspensions of silica particles the addition of emulsifier caused a statistically significant ($p<0.05$) rise in the particle size whereas the effect on HPMC suspensions was negligible. The zeta potential did not change considerably when Tween 20 was present in mixtures with silica particles however this was different when HPMC was utilised as a Pickering particle. Furthermore, the zeta potential of both particle suspensions in the presence of WPI increased towards more positive values as it was confirmed by statistical analysis ($p<0.05$).

Table 2: Z-average size, zeta potential and the corresponding span or polydispersity index (PDI) of aqueous particle suspensions and their mixtures with emulsifiers. Particle concentration was 3 wt.% in all cases. Samples annotated with a star presented more than one peaks and their particle size distribution is presented in Appendix A.

Aqueous phase	pH	Z-average size (nm)	PDI (-)	Zeta potential (mV)
Species alone				
3T	2	8.3 ± 2.4	0.19 ± 0.02	-0.21 ± 1.3
3T	6.5	8.5 ± 2.1	0.23 ± 0.02	-0.06 ± 0.9
3W*	2	206 ± 11	0.30 ± 0.03	17.9 ± 0.6
3W	6.5	18.3 ± 6.3	0.44 ± 0.09	-7.14 ± 0.3
S*	2	38.1 ± 0.5	0.25 ± 0.4	-0.02 ± 0.1
H	6.5	389 ± 12	0.45 ± 0.05	-4.5 ± 0.6
Mixed species				
S / 0.05T	2	Out of range		-0.46 ± 0.3
S / 3T	2	Out of range		0.82 ± 0.2
S / 0.05W	2	182 ± 12.1	0.55 ± 0.04	18.9 ± 0.8
S / 3W*	2	208 ± 9.8	0.34 ± 0.02	20.4 ± 0.1
H / 0.05T	6.5	404 ± 11	0.42 ± 0.18	-2.1 ± 0.4
H / 3T	6.5	409 ± 7	0.51 ± 0.05	-1.9 ± 0.3
H / 0.05W	6.5	394 ± 5	0.43 ± 0.12	-2.6 ± 0.1
H / 3W	6.5	401 ± 12	0.46 ± 0.09	-2.1 ± 0.4

3.1.1. Effect of Tween 20

Addition of Tween 20 molecules in the native silica suspension (hydrophilic particles carrying a strong negative charge) and subsequent reduction of pH to 2 resulted in extensive sedimentation. Even the presence of a small amount of Tween above CMC resulted in depletion

interaction causing the uncharged silica particles to approach and cluster. As a result, large flocs of silica particles formed and sank to the bottom of the vial. A similar mechanism is reported as effective inter-particle attraction between silica nanoparticles due to depletion interaction caused by the addition of non-ionic nonethylene glycol dodecyl ether($C_{12}E_9$) [28]. Consequently, two distinct layers appeared after a short time, a Tween 20 rich phase (clear transparent) formed at the top and a silica-rich phase (turbid sediment) at the bottom (Fig. 1). The higher the Tween 20 concentration, the stronger the depletion interaction between silica particles became. At high concentration of Tween 20 (3 wt.%) silica particles grouped in larger heavier flocs thus the thickness of the sediment layer appears smaller and denser. The large size of the particle flocs did not allow for measurement through DLS, so the size distribution data are presented in Fig. 2 as delivered through SMLS. Suspensions of silica particles containing a high concentration of Tween 20 presented large particle aggregates with an average diameter of 18.7 μm, almost double the size measured when a low concentration of Tween was used. Smaller particle size was identified for both mixtures as well at 4 μm approximately. Mixtures of silica containing 0.05 wt.% Tween 20 generated narrower distribution corresponding to a span value of 0.943 as opposed to mixtures of silica and 3 wt.% Tween 20 with a span of 1.178. The zeta potential values of the mixed silica-Tween 20 suspensions at pH 2 (Table 2) were almost equal to the silica alone (no significant difference found by statistical analysis) suggesting that no significant adsorption of Tween 20 molecules on silica particle took place.

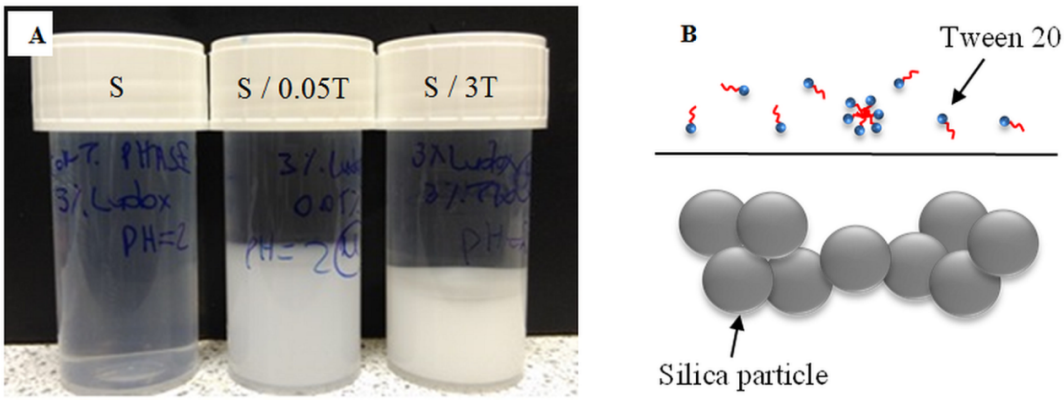

Fig. 1: (A) Aqueous suspensions of 3 wt.% silica particles alone, mixed with 0.05 wt.% and 3 wt.% Tween 20, 1 day after preparation, all at pH 2. **(B)** Schematic of the top and bottom layers of the aqueous mixtures.

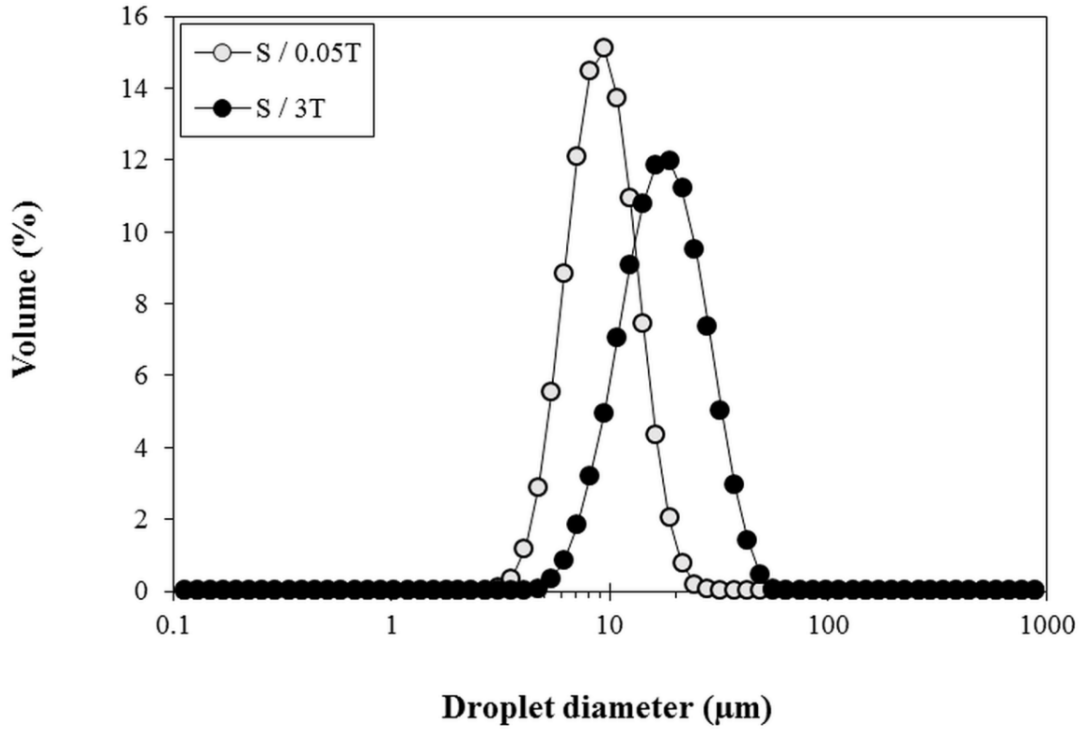

Fig. 2: Particle size of aqueous suspensions of 3 wt.% silica particles mixed with Tween 20 at pH 2.

HPMC exhibits a certain degree of hydrophobicity therefore in an aqueous environment the molecule folds and exposes its hydrophilic domains resembling the structure of a soft colloidal particle [29]. Addition of Tween to aqueous HPMC suspensions had a different effect than when silica particles were used. HPMC particles alone carried a weak negative charge at their native pH which slightly moved towards a neutral charge upon addition of Tween (Table 2). This change in the zeta potential of the HPMC particles was found statistically significant ($p<0.05$) and it could imply adsorption of Tween on the HPMC surface, however this is debatable given the minor change in the size. Indeed several studies have focused on interactions occurring in mixtures of cellulose and LMW emulsifiers though this is mainly limited to ionic surfactants [30, 31]. Admittedly, interactions between surfactant and cellulose surfaces is reported and increased surfactant concentration is associated with increased coverage of cellulose particles by surfactant molecules [32, 33]. Furthermore, it was found that the surfactant hydrophilic head group interacts with the hydrophilic cellulose surface as evidenced by atomic force microscopy [34]. A schematic representation of the possible arrangements of species in the HPMC - Tween 20 aqueous mixtures is given in Fig. 3.

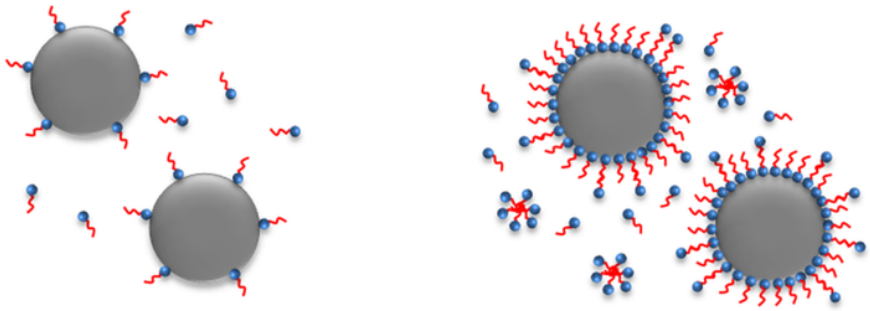

Fig. 3: Schematic representation of aqueous suspensions of 3 wt.% HPMC particles mixed with 0.05 wt.% (left) and 3 wt.% Tween 20 (right), at pH=6.5.

At low concentration of Tween 20 close to the CMC, the emulsifier molecules are sparsely distributed along the surface of HPMC particles with the hydrophobic tail protruding in the aqueous phase forming a monolayer of Tween molecules. At a high concentration of Tween (well above the CMC) the abundance of Tween molecules allows for full coating of the HPMC particles. The Tween molecules are densely packed on the particle surface and a double layer of Tween molecules may be formed due to the hydrophobic attraction between the tails of the surfactants, so this can explain the minor change in the size and the slight decrease of the net charge towards the neutral value. As a result, particle wettability could switch from hydrophilic to hydrophobic and back to hydrophilic. This scenario has been reported for mixtures of negatively charged silica particles and cationic surfactants [23], although in the case of HPMC particles and Tween 20 both species are nonpolar so electrostatic interactions are unlikely to occur.

3.1.2. Effect of WPI

WPI is an amphiphilic globular molecule and can adsorb both to hydrophobic and hydrophilic interfaces giving rise to steric interactions [35]. Unlike non-ionic Tween 20, WPI is carrying a strong charge away from its isoelectric point (IEP), that being approximately at pH values between 4.5 and 5.5. At pH values below IEP WPI carries a positive charge whereas at pH above IEP it is negatively charged [36]. This is confirmed by the zeta potential measurements (Table 2). As a result, electrostatic interactions may occur either between neighbouring proteins and/ or protein - particle surface. Stability of aqueous mixtures of particles and WPI can be affected by both steric and electrostatic interactions and the surface character of the particle should also be considered.

In Table 2 it is shown that the size of the silica particles when WPI was present at pH 2 was larger by approximately 150-170 nm compared to silica alone. Furthermore, the zeta potential of the silica particles moved from almost zero to higher positive values, demonstrating a significant change ($p<0.05$) which suggested adsorption of WPI molecules on the silica surface. During preparation of the mixed silica - WPI suspension at its native pH 10 it is possible that some WPI molecules adsorbed to silica particles despite both carrying a net negative charge. Reducing the pH closer to the IEP of the protein caused nanoparticle aggregation and the aqueous mixture became turbid. Finally, when pH reached 2 below the IEP of the protein, the WPI obtained a net positive charge and repulsive forces between the coated silica particles dominated thus the aqueous mixture became clear again (Fig. 4A). Similar observations could explain these findings for aqueous mixtures of silica particles and β- lactoglobulin in other studies, and since β- lactoglobulin is the main constituent of the WPI molecule (48 wt.% on dry basis) [37], these are reported here. In one of the studies the authors argue that despite the net negative charge of the protein at high pH, protein may reveal positive charges that appear due to the patchy distribution of the charges on the protein surface [38]. Exposure of the positive charges of WPI at high pH may appear due to the unfolding of the molecule whereas at pH lower than the IEP WPI folds [39]. As such, at high pH the protein could be electrostatically attracted to the surface of negatively charged silica particles, yet maintaining an overall net negative charge that would keep coated silica particles apart from each other and this could explain the clarity of the suspension at high pH. In another study it was shown that the aqueous mixtures of silica particles and β-lactoglobulin were stable at pH values far from the IEP while close to the IEP nanoparticle aggregation was induced due to the absence of electrostatic interactions [40] so this explains the turbidity of the suspension close to the IEP of the protein and the fact that the suspension became clear again upon further reducing pH to 2.

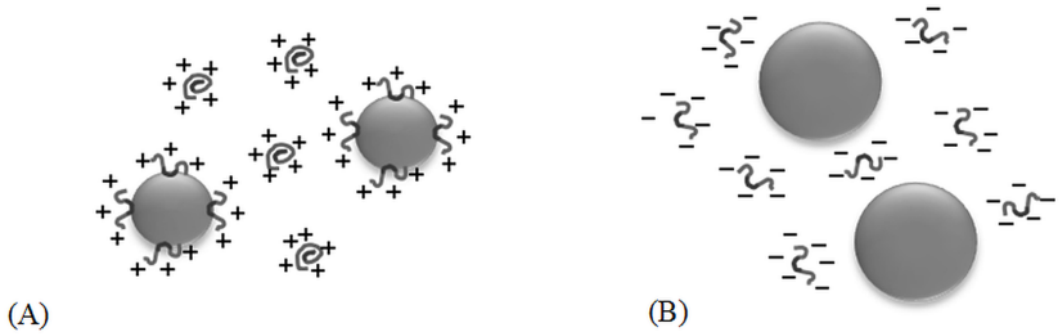

Fig. 4: Schematic representation of aqueous suspensions of WPI mixed with (A) silica at pH=2 and (B) HPMC particles at pH=6.5.

The presence of WPI in HPMC aqueous suspensions is expected to affect the behaviour of the mixture as it has been documented that mixtures of proteins and polysaccharides under certain conditions may form electrostatic complexes [41]. Moreover upon reduction of the pH to values lower than the IEP of the protein electrostatic attraction between the two biopolymers - positively charged protein and anionic polysaccharide- may occur resulting in their association forming very stable conjugates that remain soluble in the aqueous phase.

However, the pH of the studied HPMC - WPI aqueous mixtures were maintained at 6.5 above the IEP of the WPI so the formation of the complexes should be ruled out. This theory agrees with the experimental data as it is shown in Table 2 the size of the HPMC particles did not change substantially ($p>0.05$). Similar observations were highlighted for mixtures of HPMC and β-lactoglobulin as it is reported that complexation was not possible due to the negligible increase of the particle size or modification of the zeta potential [42]. Consequently, it is possible that HPMC particles and WPI molecules co-existed as separate entities in the aqueous phase with the latter interfering between HPMC particles and preventing flocculation as it is shown schematically in Fig. 4B.

3.2. Co-stabilised Pickering emulsions

3.2.1. Effect of Tween 20

Fig. 5 shows the effect of Tween 20 concentration on the droplet size and span of emulsions prepared with a fixed concentration of silica particles and varying concentrations of Tween 20 as a co-stabiliser. Emulsions stabilised with each species alone were also produced and their stability was tested throughout 3 weeks. It can be seen that silica particles alone yielded emulsions whose droplet size did not change dramatically after 21 days however an oil layer of stable thickness was present from the day of production. Despite the abundance of silica particles to coat all formed droplets, the kinetic energy of the particles was not sufficient to adsorb to the oil droplets due to the poor energy dissipation in the emulsion via the RME process (data not shown here). Another possible explanation for this could be the gradual accumulation of oil droplets within short proximity from the membrane. If this was the occasion, as emulsification continued it would be difficult for the silica particles located to the outer bulk to travel through the dense “cloud” of droplets and this could explain the oil layer that appeared by the end of emulsification.

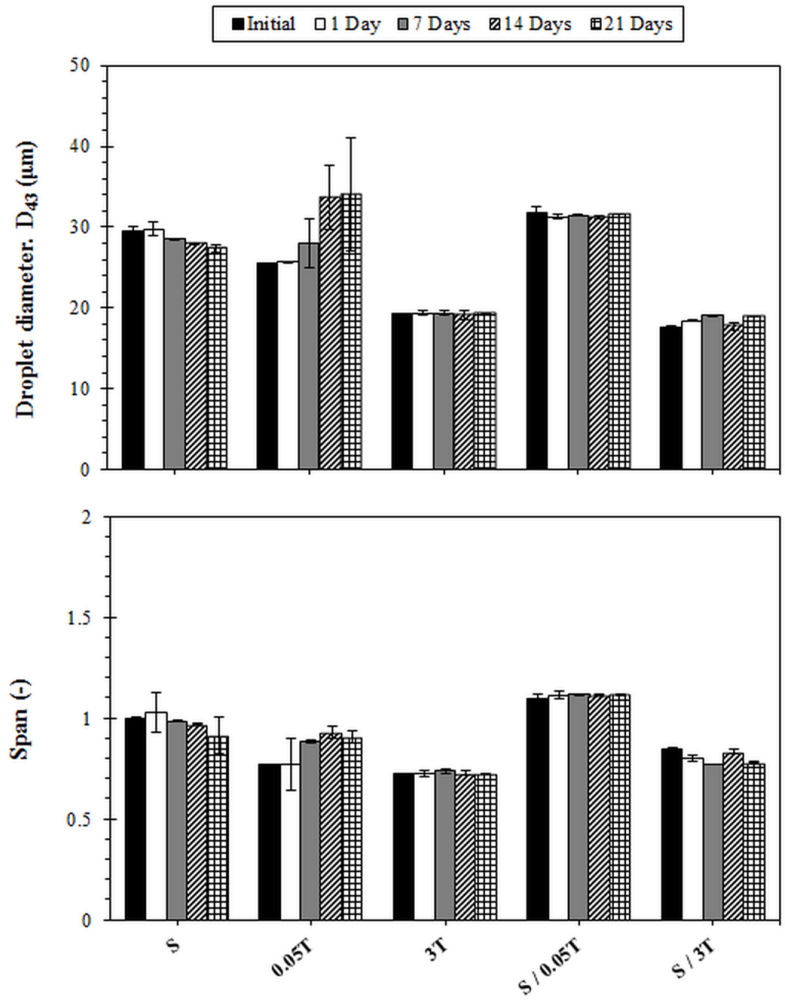

Fig. 5: Average droplet diameter and span values of emulsions stabilised with a fixed concentration of 3 wt.% silica and its mixtures with Tween 20 at pH 2. For co-stabilised emulsions, the average values account for droplets from all layers (see Fig. 6). An SPG 6.1 µm membrane was used at 10 kPa and 2000 rpm.

Compared to 3 wt.% Tween alone, emulsions stabilised with a low concentration of Tween (0.05 wt.%) presented a gradual increase in their droplet size and span that was more evident after 7 days as also indicated by the growing thickness of the oil layer that appeared following emulsification. This could be due to the rapid depletion of emulsifier at low concentration of emulsifier that caused the rate of adsorption to decrease close to the membrane surface and thus coalescence of adjacent droplets resulted in larger droplet size and width distribution. It was argued that at low concentrations of emulsifier formulation is the limiting factor and not the processing conditions [43]. Indeed a substantial increase in the droplet size and span of Tween 20 stabilised emulsions (1% oil content) through RME was found for concentrations lower than 0.2 wt. % [44].

The addition of small amount of Tween (0.05 wt.%) in the silica suspension did not have tremendous influence at the resultant droplet size of co-stabilised emulsions showing a slight increase by 2 μm compared to silica alone, however, there was a moderate increase in the span. This could be due to the presence of the two non-interacting species in the aqueous phase: flocculated silica particles and Tween 20 free molecules (see Table 2) that could trigger competitive adsorption. Competition between silica particles and non-ionic emulsifiers for adsorption to the surface of oil droplets has been discussed before suggesting that the small surfactants adsorb initially providing short-term stabilisation facilitating larger silica particles to follow [18, 45]. Because of the increased viscosity of the mixture, adsorption of Tween molecules was delayed resulting in larger droplet size compared to 0.05 wt.% Tween alone. However, the subsequent attachment of silica particles improved steric repulsion between droplets as confirmed by the extremely stable span and droplet size values after 21 days. Increasing the concentration of Tween in the mixture generated emulsions with droplet size smaller than silica alone, yet closer to the droplet size of emulsions stabilised solely by 3 wt.% Tween 20. Unsurprisingly the behaviour of these emulsions resembled that of surfactant stabilised emulsions because adsorption of the LMW emulsifiers dominated the droplet surface, excluding the adsorption of silica particles [45]. As a result of this competition, the span was kept at an intermediate level of 0.848 as opposed to 1.026 and 0.725 for silica and Tween stabilised emulsions respectively - a considerably low value to consider these emulsions fairly monodisperse. When comparing the two co-stabilised emulsions, it can also be seen that the droplet size of silica - 3 wt.% Tween emulsions was almost half the size of silica - 0.05 wt.% Tween emulsions and the span was much lower. This is attributed to the availability of the surfactant close to the membrane surface and the higher viscosity of the silica - 3 wt.% Tween mixtures contributing to higher drag forces and thus smaller droplets [22]. It is worth noting that all co-stabilised emulsions were exceptionally stable after 21 days. In particular, emulsions co-stabilised with silica and 0.05 wt.% Tween 20 were stable with no signs of coalescence and no oil layer on the top, unlike emulsions stabilised by each species alone.

It should be noted that the resultant droplet size and span values of the co-stabilised emulsions is the contribution of two populations of droplets as a consequence of the co-stabilisation mechanism the droplets undergo. After emulsification the emulsions stabilised by silica - Tween mixtures formed gradually three layers: a cream layer on the top of the emulsions, a clear serum and a sediment at the bottom of the sample pot. This agrees with studies showing that sedimentation occurred for emulsions stabilised by mixtures of silica particles and non-

ionic emulsifier due to flocculation of silica particles upon addition of surfactant [18]. Excluding the cream layer, the appearance of these emulsions was similar to the silica - Tween aqueous suspensions because of the large size of the silica flocs (Table 2 & Fig. 2). However, in this case both the cream and sediment contained droplets as it is shown in the micrographs (Fig. 6). Cream layer was denser containing more droplets that were strongly flocculated as opposed to droplets residing at the bottom and this is reported elsewhere [22]. Therefore it was suggested that the creamy layer consisted primarily of droplets stabilised by Tween whereas flocs of silica particles dominated on the surface of oil droplets at the bottom layer. As it is shown by the droplet size distribution, droplets of similar size existed at both layers however smaller sizes were picked up by DLS measurements from the bottom layer due to the presence of free silica aggregates and that also explains the larger span value. To confirm this, oil droplets stabilised by mixtures of silica-Tween were visualised through Cryo-SEM and their surface morphology was compared with those stabilised by either of the species alone. Fig. 7A-B shows an oil droplet stabilised solely by silica particles whose surface is clearly occupied by flocs of small silica particles in very close packing with size comparable to our findings (Table 2). The surface of this droplet shows some irregularities when compared to the solely Tween stabilised droplet which has a smoother surface (Fig. 7C). These 'wrinkles' have been previously suggested to indicate the presence of particles at the oil-water interfaces [46]. In order to clearly visualise oil droplets through Cryo-SEM most of the water was removed by freeze fracturing of emulsion samples and this was followed by dusting the samples with gold particles under vacuum. It is this process that generated large pressure gradients and caused the particle-stabilised droplets to appear a corrugated surface [47]. Collapsing of a monolayer of particles adsorbed on the oil-water interface, also reported as 'buckling', took place when surface pressure equalised with the interfacial tension of oil/water [48]. Presumably, a small amount of oil can escape making the total surface area of droplets smaller so the strongly adsorbed particles compress in order to cover a smaller area. This is clearly seen in Fig. 7E & G where droplets from the bottom layer of co-stabilised emulsions presented wrinkles alongside their surface. On the contrary droplets from the creamy layer had a different morphology and their surface appeared smoother (Fig. 7D & F). Hence the top layer consisted of drops stabilised mainly by Tween while the sediment contained mainly drops stabilised by silica particles.

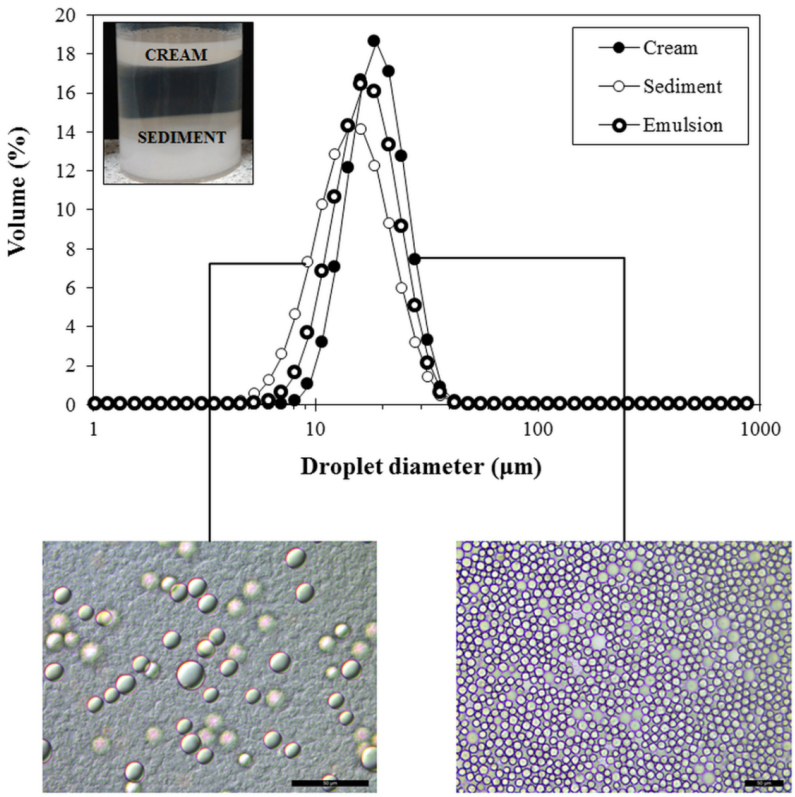

Fig. 6: Droplet size distribution of emulsion co-stabilised with 3 wt.% silica and 3 wt.% Tween 20 at pH 2 after 1 day. Micrographs were taken from the cream and the sediment layer of the emulsion. The scale is 50 µm in all cases.

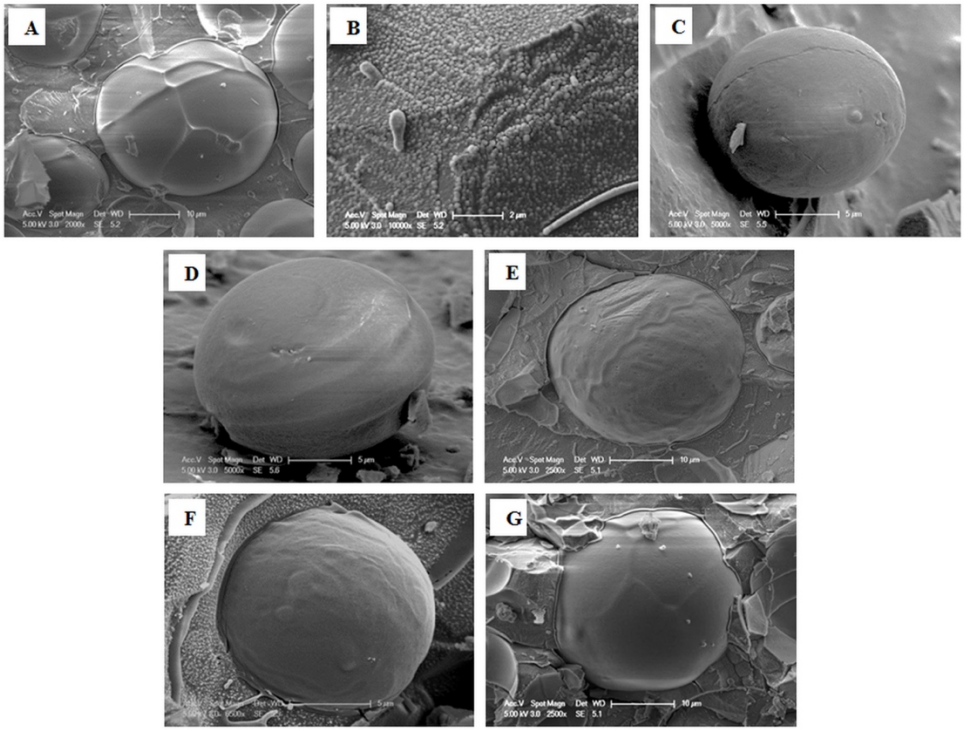

Fig. 7: Cryo-SEM micrographs of emulsion droplets stabilised by 3 wt.% silica alone with a close-up of the droplet surface (A-B), 3 wt.% Tween 20 alone (C), 3 wt.% silica mixed with 0.05 wt. % Tween 20 top and bottom layer (D-E), 3 wt.% silica mixed with 3 wt.% Tween 20 top and bottom layer (F-G). All emulsions were produced by an SPG 6.1 µm at 10 kPa and 2000 rpm. All pictures were taken 3 days following emulsification.

The effect of the concentration of Tween20 on the droplet size and span of emulsions co-stabilised with mixtures of HPMC and Tween and adjusted at pH 6.5 is shown in Fig. 8 for a period of 21 days. Emulsions prepared using HPMC alone phase separated completely within a short time after production and therefore no further stability data are presented. These results correlate with data showing that emulsions produced by cellulose nanocrystals were unstable in the absence of surfactant [49]. Furthermore, it was shown that due to the low energy dissipation via RME the kinetic energy of this particle close to the membrane surface was not sufficient to induce an energy barrier for adsorption (data not shown here).

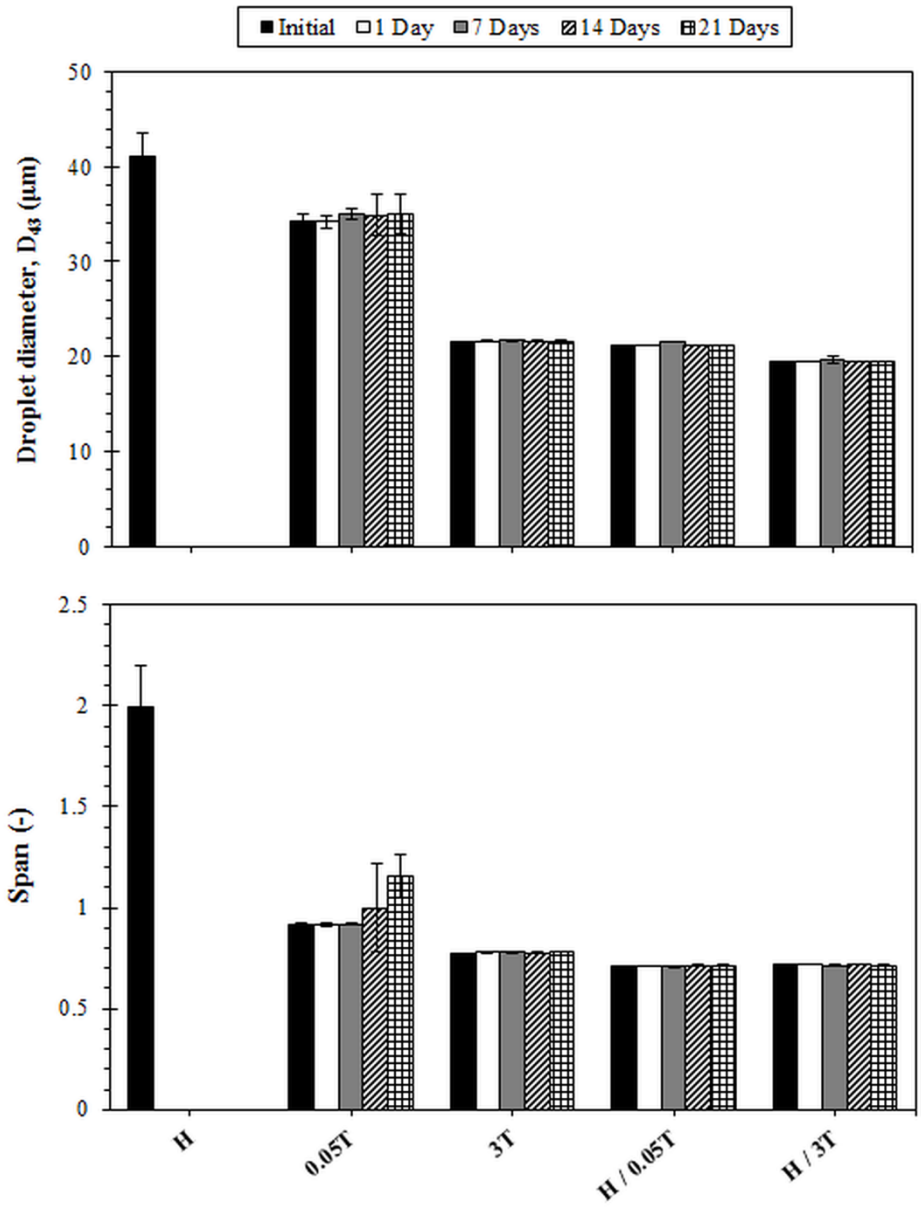

Fig. 8: Average droplet diameter and span values of emulsions stabilised with 3 wt.% HPMC and its mixtures with Tween 20 at pH 6.5. An SPG 6.1 µm membrane was used at 10 kPa and 2000 rpm.

For freshly produced emulsions containing 0.05 wt.% Tween 20 at pH 6.5, the droplet size and the span were found larger compared to the same emulsions prepared at pH 2. Although in general non-ionic emulsifiers are considered to be pH insensitive, it is reported that the hydration rate of Tween molecules (initial concentration 0.02%) dissolved in aqueous medium at pH 2 was almost four times higher than pH 6.5 [50]. Furthermore in another study it was shown that increasing the pH of non-ionic Tween 40 would cause less hydration per unit mass of surfactant and the critical micelle concentration is decreased considerably which means more surfactant micelles in the aqueous solution [51]. Consequently, it is possible that the availability of Tween molecules for adsorption at low pH was increased causing faster reduction of the interfacial tension and thus smaller drops. This effect was not pronounced at higher concentrations of surfactant therefore droplet size and span of Tween only stabilised emulsions were similar at both pH values. As expected, low concentration of emulsifier led to droplet coalescence after production as reflected by the slight increase in the drop size and the significant increase in the span from 0.914 to 1.159 after 21 days whereas high concentration of emulsifier resulted in stable emulsions with 12 μm smaller droplet size and very narrow distribution.

The presence of low concentration of Tween 20 in mixtures with HPMC allowed for the formation of co-stabilised emulsions with a remarkably smaller droplet size and span than emulsions stabilised by single species. Specifically, the droplet size of co-stabilised emulsion appeared 50% and 40% smaller than emulsions stabilised by HPMC alone and 0.05% Tween alone respectively. This behaviour is a typical example of the synergistic effect exhibited by the co-existence of two emulsifying agents in emulsions and has been reported for mixtures of small molecular surfactants with inorganic (silica) as well as other edible Pickering particulate structures (e.g. cellulose nanocrystals) [49, 52]. HPMC particles benefit from their interaction with the LMW emulsifiers (Table 2) rendering them partially hydrophobic, thereby enhancing their affinity to the oil surface. The co-stabilised emulsions were very monodisperse demonstrating a span of approximately 0.71 which is indicative of their robust stabilisation by HPMC particles. A similar system encompassing HPMC and Tween 80 has been found to operate in the same fashion [21]. The authors describe a surfactant-limiting co-stabilisation mechanism, clearly underlying the effect of surfactant concentration on the resultant droplet size and ultimate stability. They found that by increasing surfactant concentration considerably smaller droplets were produced as a consequence of the dominance of Tween molecules at the interface and their ability to induce droplet breakup. This is in contrast with our findings as it

was observed that even at a higher emulsifier concentration (3 wt.%) the droplet size and span of co-stabilised emulsions remained practically the same.

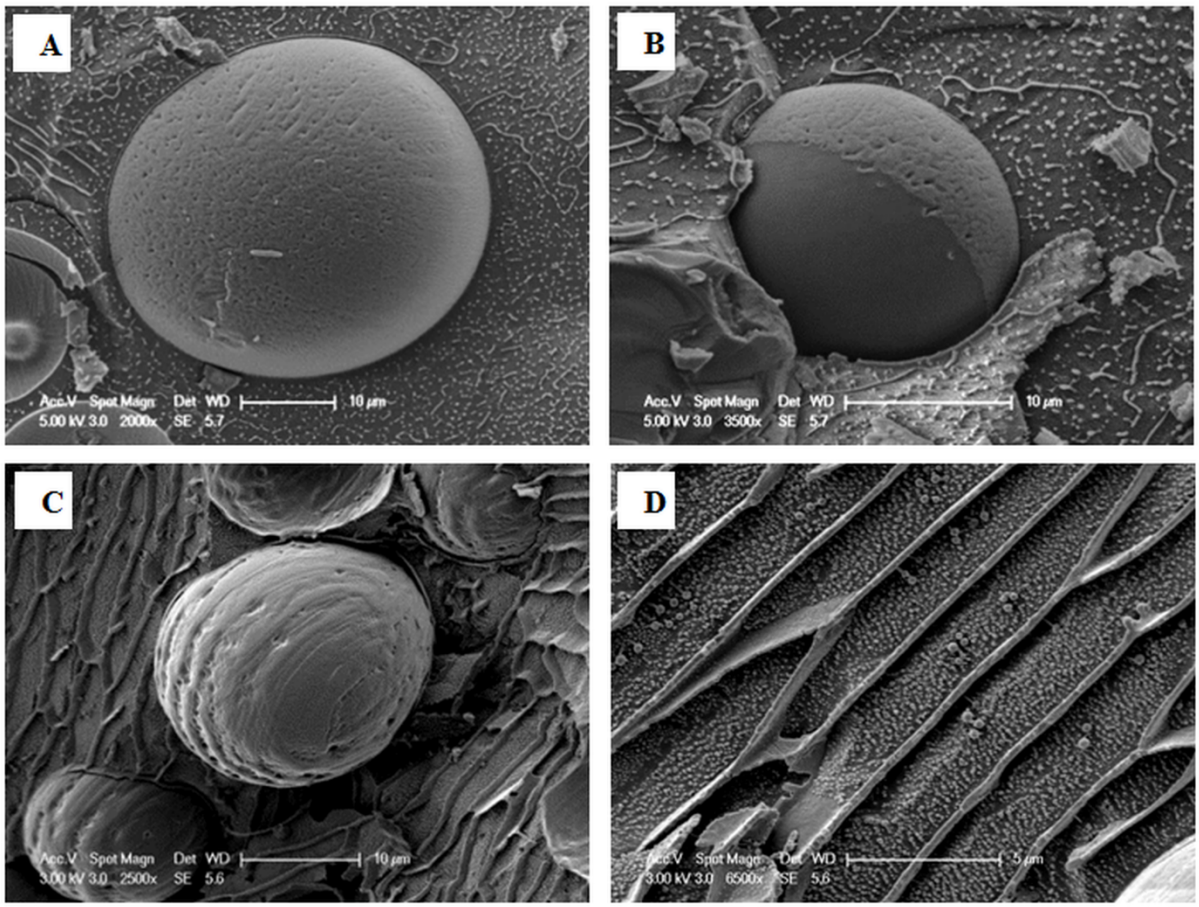

Fig. 9: Cryo-SEM micrographs of emulsion droplets stabilised by 3 wt.% HPMC mixed with (A-B) 0.05 wt.% Tween 20, (C-D) 3 wt.% Tween with a close-up of the aqueous phase gel network. All emulsions were produced by an SPG 6.1 μm at 10 kPa and 2000 rpm.

This could be ascribed to the different structuring of the aqueous phase upon increasing Tween concentration as it can be seen in Fig. 9. At low emulsifier concentration small particle aggregates were visible in the aqueous phase and on the droplet surface (Fig. 9A-B). This is in accordance with findings reporting that aggregates of cellulose nanocrystals and surfactant were sighted on the surface of PMMA particles [53]. Upon increasing of Tween concentration a gel network formed in the aqueous phase as shown in Fig. 9C. Formation of gel network has been reported for mixtures of non-ionic polymers and surfactants as interactions become significant when surfactant concentration reaches the critical aggregation concentration value [33]. More specifically, it is possible that the presence of more emulsifiers could cause HPMC

particles to turn back to hydrophilic as new Tween20 molecules deposited on the existed emulsifier layer with the head groups exposed in the aqueous phase (see Fig. 3B) thereby decreasing their affinity for the oil droplet surface. Consequently, the oil droplets were occupied by the free Tween20 whereas the association of the excluded HPMC particles coupled with less amount of water in the aqueous phase led to the formation of a gel network as it is seen in Fig. 9D. The increased viscosity of the gel network prevented collision of droplets and enhanced stability of emulsions, confirmed by the low span (0.717) that was very similar to HPMC - 0.05% Tween emulsions. Despite exhibiting different stabilisation mechanisms, very monodisperse small sized co-stabilised emulsions were produced by both concentrations of Tween20 as a result of the use of the rotating membrane.

3.2.2. Effect of WPI

Fig. 10 illustrates the droplet size and span values of emulsions co-stabilised by silica particles and two concentrations of WPI and their stability after 21 days. For convenience, emulsions stabilised solely by silica are plotted again in order to facilitate comparisons and trends between the samples. Focusing on the systems with single WPI a similar trend can be distinguished with the Tween only stabilised emulsion; that is the reduction of the droplet size and span with increasing concentration of emulsifier. High concentration of emulsifier (3 wt.%) resulted in higher availability of emulsifiers close to the membrane surface causing faster decrease in the interfacial tension and as a consequence smaller droplet size and span values after 21 days. To our knowledge there are not available literature findings for WPI stabilised emulsions prepared by membrane emulsification therefore sodium caseinate is mentioned here as reference as it is a milk protein, yet it has a random coil structure so it is likely that it would behave differently during adsorption to oil-water interface compared to the globular WPI. It was reported that for SPG membrane at constant transmembrane pressure and rotational velocity, the droplet size of emulsions stabilised by sodium caseinate reduced upon increasing concentration of the protein from 0.1% to 3% whereas the droplet size distribution became narrower [54]. Because WPI is an HMW emulsifier transfer of the molecule to the oil-water interface was considerably slower than smaller Tween 20 and as a result the interfacial tension decreased at a slower rate. Hence low concentration of WPI (0.05 wt.%) in the aqueous phase generated larger droplets than same concentration of Tween 20. In contrast at high concentration of emulsifier this effect was counteracted by the larger availability of emulsifier, and as a consequence, the droplet size and

span values were very similar for both species. Therefore in this case droplet size appears to be governed by processing conditions rather than formulation-specific circumstances.

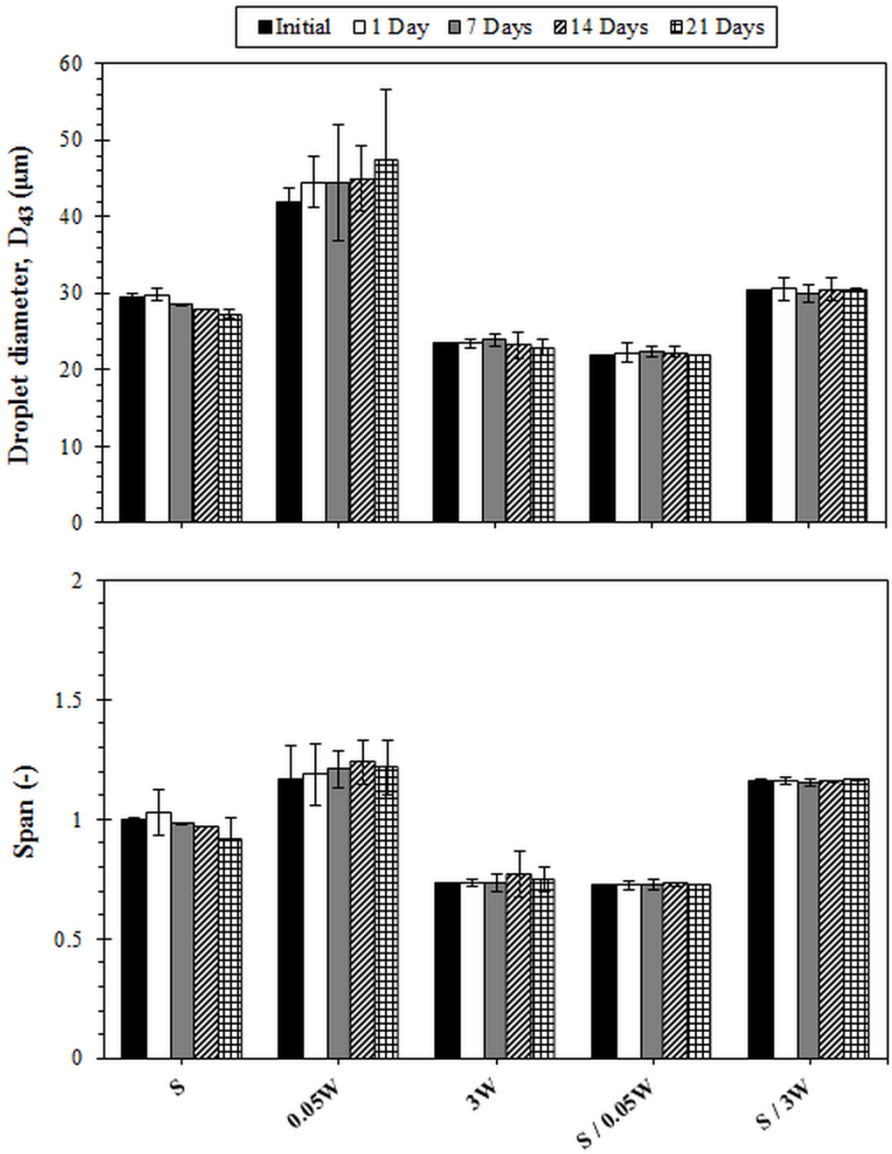

Fig. 10: Average droplet diameter and span values of emulsions stabilised with 3 wt.% silica and its mixtures with WPI at pH 2. An SPG 6.1 µm membrane was used at 10 kPa and 2000 rpm.

As mentioned previously emulsions prepared with silica particles alone presented coalescence at a certain degree which was also the case for the emulsions made with 0.05 wt. % only. However, the presence of low concentration of WPI in the aqueous suspension of silica particles at pH 2 resulted in emulsions with droplet size that was 24% than silica alone and a span as low as 0.725. Certainly, both values were far smaller than systems whose aqueous

phase included only 0.05 wt.% WPI. The emulsions showed remarkable stability throughout the entire period of 21 days as indicated by the minor changes in their droplet size and span values. This behaviour could be related to the adsorption of WPI monomers on the silica surface rendering them more hydrophobic whilst surrounded by a positive charge (Fig. 4A). It is suggested that the modified silica particles were able to effectively decrease interfacial tension thus forming smaller droplets than silica particles alone whilst providing effective stabilisation through steric and electrostatic repulsion between neighbouring droplets. The synergy between silica particles and β-lactoglobulin has been confirmed in the case of long-term stabilisation of foams [55]. In this study, it was found that the extent of Ostwald ripening was considerably delayed compared to the pure protein systems owing to an increase in the interfacial elasticity as delivered by the adsorbed protein so the same mechanism could also apply in our system and could be responsible for the remarkable stability of the investigated emulsions. Furthermore, it is possible that silica particles could be entrapped in the viscoelastic thin film created by the adsorbed proteins thereof constituting an additional layer that provides additional repulsive forces between droplets [56]. In a separate study, instead of β-lactoglobulin another milk protein sodium caseinate was used in mixtures with silica to show that significant reduction in the interfacial tension between oil-water took place when both species were present in the aqueous phase [45]. Surprisingly, high concentration of WPI in mixtures with silica particles yielded polydisperse emulsions with droplet size larger than when species were used alone. This could be associated with the increased viscosity of the aqueous mixture when high concentrations of WPI are present as the transfer of the emulsifier towards the oil-water interface is substantially lowered. At the same time due to higher viscosity, the newly generated droplets cannot move away from the membrane surface therefore the probability of coalescence was increased [25].

Emulsions prepared with HPMC-WPI mixtures exhibited very similar behaviour to the silica-Tween systems owing to the weak interactions between particles and co-stabilisers in the bulk that could signify competitive adsorption between the individual species. However unmodified HPMC particles are too hydrophilic to adsorb to the oil-water interface, and this was confirmed by complete phase separation of emulsions stabilised with HPMC alone shortly after emulsification. Therefore it was expected that WPI would dictate adsorption. As it is seen in Fig. 11 the presence of low concentration of WPI in the aqueous mixture resulted in emulsions with similar droplet size to emulsions prepared with 0.05 wt.% WPI alone and their stability was also poor as it is shown by the dramatic increase in both the droplet size and the span

particularly that was apparent from day 1. Previous studies in mixtures of HPMC and β-lactoglobulin confirm this hypothesis [42]. In this work, although a more hydrophobic type of HPMC has been used in conjunction with β-lactoglobulin it was documented that the protein dominates the oil-water interface as evidenced by the surface pressure measurements. The HPMC exclusion as it is mentioned occurred at pH 6 and the emulsions were characterised by a thin viscoelastic film which was indicative of WPI adsorption. This was also observed in our results as with the presence of high concentration of WPI in the mixture, emulsions appeared to have 51% smaller droplet size and approximately 50% smaller span than emulsions stabilised by these species alone. Although no significant interactions took place between HPMC particles and WPI molecules, the possibility of formation of a weak gel network as a result of induced particle flocculation in the aqueous phase should not be ruled out, especially in the presence of high concentration of WPI that could explain the narrow droplet size distribution of emulsions stabilised by HPMC and 3 wt.% WPI via rotating membrane emulsification.

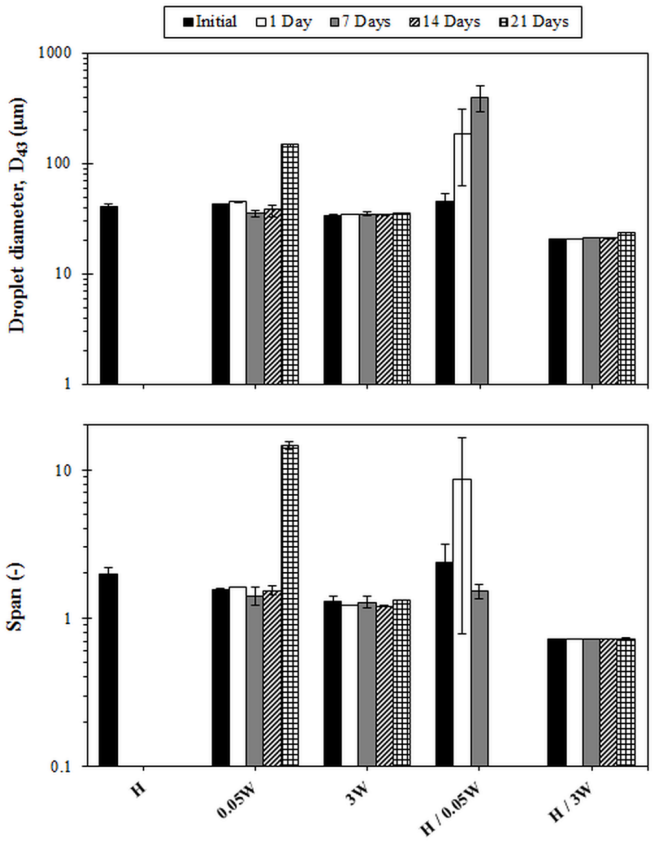

Fig. 11: Average droplet diameter and span values of emulsions stabilised with 3 wt.% HPMC and its mixtures with WPI at pH 6.5. An SPG 6.1 μm membrane was used at 10 kPa and 2000 rpm.

4. Conclusions

The effect of colloidal particle type and size as well as the concentration and type of emulsifier has been demonstrated for the production of co-stabilised O/W Pickering emulsions with enhanced stability to coalescence, via rotating membrane emulsification. The bulk and interfacial behaviour of the aqueous particle-emulsifier mixtures was related to the resultant emulsion microstructure. Due to the low energy profile of the process, adsorption of colloidal particles to the oil-water interface was not encouraged, thereby yielding unstable emulsions. The synergism occurred when a low concentration of emulsifier adsorbed on particles, resulted in co-stabilised Pickering emulsions that were stable to coalescence with smaller droplets and lower polydispersity than emulsions prepared with either of the two species alone at the same concentration. When adsorption of emulsifier on particles did not occur, species behaved as individual entities and competed to the surface of droplets. Hence, at low emulsifier concentration, silica-Tween 20 emulsions presented larger droplet size than those prepared by each species alone whereas emulsification failed for mixtures of HPMC and WPI. Upon increase of emulsifier concentration the oil droplet surface was dominated by the emulsifier and the increased viscosity of the aqueous particle-emulsifier mixture contributed to even smaller droplet size than emulsions stabilised solely with emulsifier. Notably, the exclusion of HPMC particles from the oil-water interface resulted in extra-stable monodisperse emulsions via the establishment of a weak gel network due to the depletion flocculation in the presence of high emulsifier concentrations. Depending on the surface chemistry of a particle, WPI could be a good alternative to Tween 20 to make stable Pickering emulsions via rotating membrane emulsification, as it can be used in low concentrations to achieve comparable results. The positioning of all species in the continuous phase rather than the internal oil phase suggests a feasible strategy for minimisation of internal fouling of the membrane that could improve production rates. In this context, rotating membrane emulsification offers a viable alternative to traditional techniques for development of well-controlled edible microstructures that could be incorporated in foods as well as pharmaceuticals for example for controlled release of flavours or nutrients or targeted drug delivery purposes.

Acknowledgements

The authors acknowledge Eamon Ridgley and Nicholas Salford for performing preliminary experiments. This research was funded by the Centre for Innovative Manufacturing in Food (CIM) and the Engineering and Physical Sciences Research Council (EP/K030957/1).

Appendix A

1. Viscosities of aqueous phases

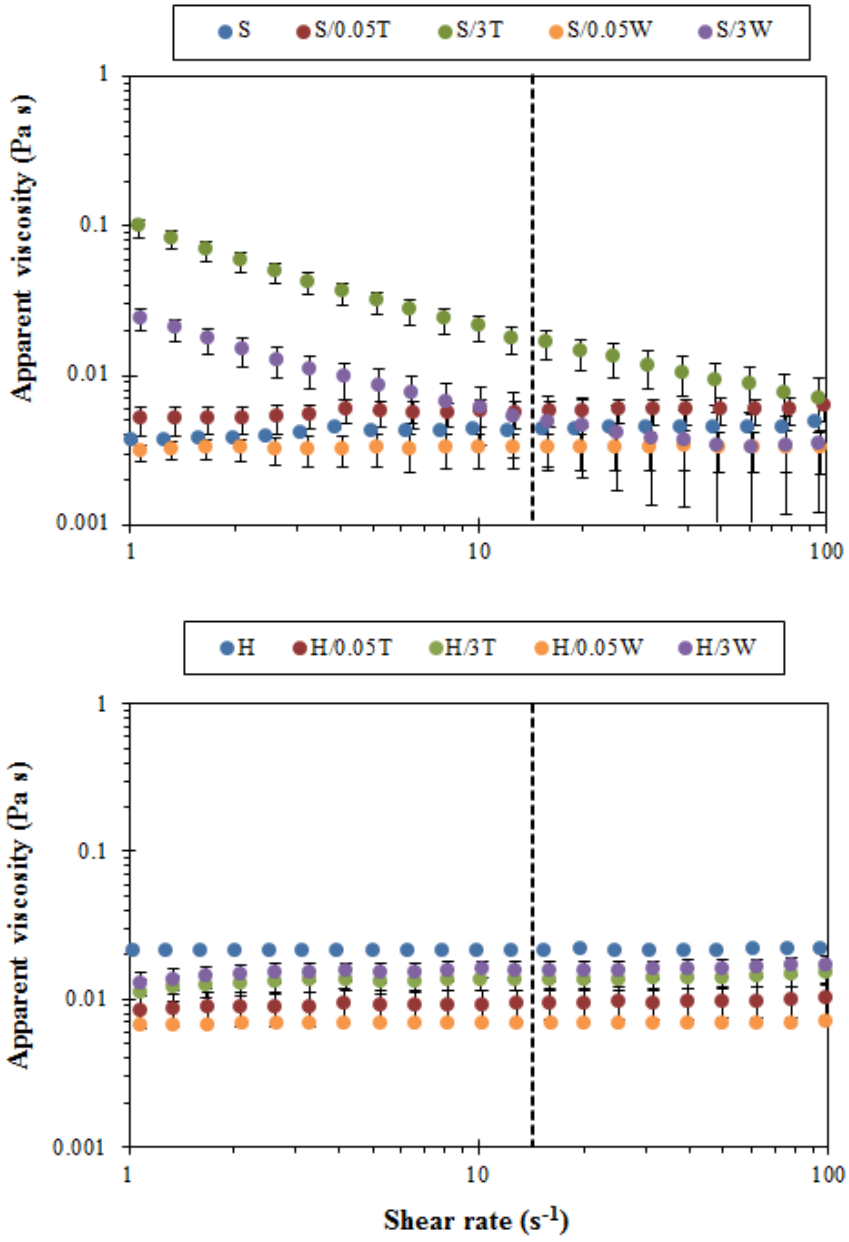

Fig. A.1: Viscosity as a function of shear rate for aqueous suspensions of particles and their mixtures with emulsifier (top: silica suspensions at pH 2 and bottom: HPMC suspensions at pH 6.5). The dotted line represents the fixed shear rate at the membrane surface used in this study (14 s^{-1}).

2. Particle size distributions

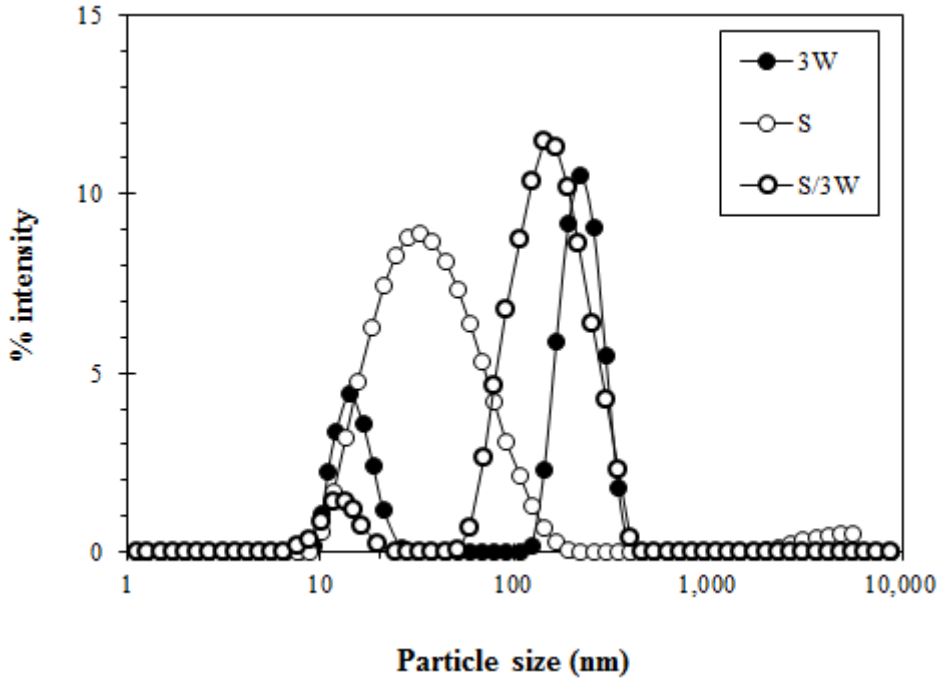

Fig. A.2: Particle size distribution of aqueous phases as obtained from DLS, all prepared at pH=2. Each curve represents the average of three subsequent measurements.

References

1. McClements, D.J., *Food emulsions: principles, practices, and techniques*. 2004: CRC press.
2. Friberg, S., K. Larsson, and J. Sjoblom, *Food emulsions*. 2003: CRC Press.
3. Schubert, H. and H. Karbstein, *Mechanical emulsification*, in *Developments in Food Engineering*. 1994, Springer. p. 9-14.
4. Nakashima, T., *Membrane emulsification by microporous glass.* Key Eng. Mater., 1991. **61**: p. 513-516.
5. Spyropoulos, F., et al., *Advances in membrane emulsification. Part B: recent developments in modelling and scale-up approaches.* Journal of the science of food and agriculture, 2014. **94**(4): p. 628-638.
6. Vladisavljević, G.T. and R.A. Williams, *Manufacture of large uniform droplets using rotating membrane emulsification.* Journal of colloid and interface science, 2006. **299**(1): p. 396-402.
7. Piacentini, E., E. Drioli, and L. Giorno, *Membrane emulsification technology: Twenty-five years of inventions and research through patent survey.* Journal of Membrane Science, 2014. **468**: p. 410-422.
8. Spyropoulos, F., et al., *Advances in membrane emulsification. Part A: recent developments in processing aspects and microstructural design approaches.* Journal of the science of food and agriculture, 2014. **94**(4): p. 613-627.
9. Berton-Carabin, C.C. and K. Schroën, *Pickering emulsions for food applications: background, trends, and challenges.* Annual review of food science and technology, 2015. **6**: p. 263-297.
10. Zafeiri, I., et al., *The role of surface active species in the fabrication and functionality of edible solid lipid particles.* Journal of colloid and interface science, 2017. **500**: p. 228-240.
11. Duffus, L.J., et al., *A comparative study on the capacity of a range of food-grade particles to form stable O/W and W/O Pickering emulsions.* Journal of colloid and interface science, 2016. **473**: p. 9-21.
12. Rayner, M., et al., *Quinoa starch granules as stabilizing particles for production of Pickering emulsions.* Faraday discussions, 2012. **158**(1): p. 139-155.
13. Tcholakova, S., N. Denkov, and A. Lips, *Comparison of solid particles, globular proteins and surfactants as emulsifiers.* Physical Chemistry Chemical Physics, 2008. **10**(12): p. 1608-1627.
14. Salari, J.W., et al., *Deformation of the water/oil interface during the adsorption of sterically stabilized particles.* Langmuir, 2014. **30**(25): p. 7327-7333.
15. Leal-Calderon, F. and V. Schmitt, *Solid-stabilized emulsions.* Current Opinion in Colloid & Interface Science, 2008. **13**(4): p. 217-227.
16. Yuan, Q., et al., *Preparation of particle-stabilized emulsions using membrane emulsification.* Soft Matter, 2010. **6**(7): p. 1580-1588.
17. Manga, M.S., et al., *Production of solid-stabilised emulsions through rotational membrane emulsification: influence of particle adsorption kinetics.* Soft Matter, 2012. **8**(5): p. 1532-1538.
18. Zou, S., et al., *Synergistic stabilization and tunable structures of Pickering high internal phase emulsions by nanoparticles and surfactants.* Colloids and Surfaces A: Physicochemical and Engineering Aspects, 2013. **436**: p. 1-9.
19. Santini, E., et al., *Emulsions stabilized by the interaction of silica nanoparticles and palmitic acid at the water–hexane interface.* Colloids and Surfaces A: Physicochemical and Engineering Aspects, 2014. **460**: p. 333-341.
20. Pichot, R., F. Spyropoulos, and I.T. Norton, *O/W emulsions stabilised by both low molecular weight surfactants and colloidal particles: The effect of surfactant type and concentration.* Journal of Colloid and Interface Science, 2010. **352**(1): p. 128-135.
21. Zafeiri, I., et al., *Emulsions Co-Stabilised by Edible Pickering Particles and Surfactants: The Effect of HLB Value.* Colloid and Interface Science Communications, 2017(17): p. 5-9.

22. Yuan, Q. and R.A. Williams, *CO-stabilisation mechanisms of nanoparticles and surfactants in Pickering Emulsions produced by membrane emulsification.* Journal of Membrane Science, 2016. **497**: p. 221-228.
23. Binks, B.P., J.A. Rodrigues, and W.J. Frith, *Synergistic interaction in emulsions stabilized by a mixture of silica nanoparticles and cationic surfactant.* Langmuir, 2007. **23**(7): p. 3626-3636.
24. Schulz, M.B. and R. Daniels, *Hydroxypropylmethylcellulose (HPMC) as emulsifier for submicron emulsions: influence of molecular weight and substitution type on the droplet size after high-pressure homogenization.* European Journal of Pharmaceutics and Biopharmaceutics, 2000. **49**(3): p. 231-236.
25. Lloyd, D.M., I.T. Norton, and F. Spyropoulos, *Processing effects during rotating membrane emulsification.* Journal of Membrane Science, 2014. **466**(0): p. 8-17.
26. Kukizaki, M., *Microbubble formation using asymmetric Shirasu porous glass (SPG) membranes and porous ceramic membranes—A comparative study.* Colloids and Surfaces A: Physicochemical and Engineering Aspects, 2009. **340**(1-3): p. 20-32.
27. Dickinson, E., *Food emulsions and foams: Stabilization by particles.* Current Opinion in Colloid & Interface Science, 2010. **15**(1–2): p. 40-49.
28. Sharma, K.P., V.K. Aswal, and G. Kumaraswamy, *Adsorption of nonionic surfactant on silica nanoparticles: structure and resultant interparticle interactions.* The Journal of Physical Chemistry B, 2010. **114**(34): p. 10986-10994.
29. Camino, N.A., et al., *Hydroxypropylmethylcellulose at the oil–water interface. Part I. Bulk behaviour and dynamic adsorption as affected by pH.* Food Hydrocolloids, 2011. **25**(1): p. 1-11.
30. Penfold, J., et al., *Surfactant adsorption onto cellulose surfaces.* Langmuir, 2007. **23**(16): p. 8357-8364.
31. Avranas, A. and V. Tasopoulos, *Aqueous solutions of sodium deoxycholate and hydroxypropylmethylcellulose: dynamic surface tension measurements.* Journal of colloid and interface science, 2000. **221**(2): p. 223-229.
32. Manousakis, M. and A. Avranas, *Dynamic surface tension studies of mixtures of hydroxypropylmethylcellulose with the double chain cationic surfactants didodecyldimethylammonium bromide and ditetradecyldimethylammonium bromide.* Journal of colloid and interface science, 2013. **402**: p. 237-245.
33. Joshi, S.C., *Sol-gel behavior of hydroxypropyl methylcellulose (HPMC) in ionic media including drug release.* Materials, 2011. **4**(10): p. 1861-1905.
34. Singh, S.K. and S.M. Notley, *Adsorption of Nonionic Surfactants (C n E m) at the Silica− Water and Cellulose− Water Interface.* The Journal of Physical Chemistry B, 2010. **114**(46): p. 14977-14982.
35. McClements, D.J., *Food emulsions: principles, practices, and techniques*. 2015: CRC press.
36. Pelegrine, D. and C. Gasparetto, *Whey proteins solubility as function of temperature and pH.* LWT-Food Science and Technology, 2005. **38**(1): p. 77-80.
37. Kilara, A. and M. Vaghela, *Whey proteins*, in *Proteins in food processing*. 2004, Woodhead Publishing, Cambridge, England. p. 72-99.
38. Meissner, J., et al., *Characterization of protein adsorption onto silica nanoparticles: influence of pH and ionic strength.* Colloid and polymer science, 2015. **293**(11): p. 3381-3391.
39. Monahan, F.J., J.B. German, and J.E. Kinsella, *Effect of pH and temperature on protein unfolding and thiol/disulfide interchange reactions during heat-induced gelation of whey proteins.* Journal of Agricultural and Food Chemistry, 1995. **43**(1): p. 46-52.
40. Wu, X. and G. Narsimhan, *Characterization of secondary and tertiary conformational changes of β-lactoglobulin adsorbed on silica nanoparticle surfaces.* Langmuir, 2008. **24**(9): p. 4989-4998.

41. Benichou, A., et al., *Formation and characterization of amphiphilic conjugates of whey protein isolate (WPI)/xanthan to improve surface activity.* Food Hydrocolloids, 2007. **21**(3): p. 379-391.
42. Camino, N.A., et al., *Hydroxypropylmethylcellulose–β-lactoglobulin mixtures at the oil–water interface. Bulk, interfacial and emulsification behavior as affected by pH.* Food Hydrocolloids, 2012. **27**(2): p. 464-474.
43. Hancocks, R.D., F. Spyropoulos, and I.T. Norton, *Comparisons between membranes for use in cross flow membrane emulsification.* Journal of Food Engineering, 2013. **116**(2): p. 382-389.
44. Hancocks, R., F. Spyropoulos, and I. Norton, *The effects of membrane composition and morphology on the rotating membrane emulsification technique for food grade emulsions.* Journal of Membrane Science, 2016. **497**: p. 29-35.
45. Pichot, R., F. Spyropoulos, and I.T. Norton, *Competitive adsorption of surfactants and hydrophilic silica particles at the oil–water interface: Interfacial tension and contact angle studies.* Journal of Colloid and Interface Science, 2012. **377**(1): p. 396-405.
46. Ngai, T. and S.A. Bon, *Particle-stabilized emulsions and colloids: formation and applications*. 2014: Royal Society of Chemistry.
47. Jones, J.R., et al., *Effect of processing variables and bulk composition on the surface composition of spray dried powders of a model food system.* Journal of Food Engineering, 2013. **118**(1): p. 19-30.
48. Aveyard, R., et al., *Structure and collapse of particle monolayers under lateral pressure at the octane/aqueous surfactant solution interface.* Langmuir, 2000. **16**(23): p. 8820-8828.
49. Hu, Z., et al., *Surfactant-enhanced cellulose nanocrystal Pickering emulsions.* Journal of colloid and interface science, 2015. **439**: p. 139-148.
50. BATES, T.R., C.H. NIGHTINGALE, and E. DIXON, *Kinetics of hydrolysis of polyoxyethylene (20) sorbitan fatty acid ester surfactants.* Journal of Pharmacy and Pharmacology, 1973. **25**(6): p. 470-477.
51. Bloor, J., J. Morrison, and C. Rhodes, *Effect of pH on the micellar properties of a nonionic surfactant.* Journal of pharmaceutical sciences, 1970. **59**(3): p. 387-391.
52. Pichot, R., F. Spyropoulos, and I.T. Norton, *Mixed-emulsifier stabilised emulsions: Investigation of the effect of monoolein and hydrophilic silica particle mixtures on the stability against coalescence.* Journal of Colloid and Interface Science, 2009. **329**(2): p. 284-291.
53. Kedzior, S.A., H.S. Marway, and E.D. Cranston, *Tailoring cellulose nanocrystal and surfactant behavior in miniemulsion polymerization.* Macromolecules, 2017. **50**(7): p. 2645-2655.
54. Christov, N.C., et al., *Capillary mechanisms in membrane emulsification: oil-in-water emulsions stabilized by Tween 20 and milk proteins.* Colloids and Surfaces A: Physicochemical and Engineering Aspects, 2002. **209**(1): p. 83-104.
55. Kostakis, T., R. Ettelaie, and B.S. Murray, *Enhancement of stability of bubbles to disproportionation using hydrophilic silica particles mixed with surfactants or proteins.* Food colloids: Self-assembly and material science, 2007: p. 357e368.
56. Sethumadhavan, G.N., A. Nikolov, and D. Wasan, *Film stratification in the presence of colloidal particles.* Langmuir, 2001. **17**(7): p. 2059-2062.